Published in final edited form as:
Biochem Biophys Res Commun. 2014 April 25; 447(1): 26–31. doi:10.1016/j.bbrc.2014.03.068.

A new protein fold in human FKBP25/FKBP3 and HectD1

Sara Helander[#1], **Meri Montecchio**[#1], **Alexander Lemak**[2], **Christophe Farès**[2,7], **Jonas Almlöf**[1,6], **Yanjun Yi**[3], **Adelinda Yee**[2], **Cheryl Arrowsmith**[3,4], **Sirano DhePaganon**[3,5], and **Maria Sunnerhagen**[1,*]

[1] Department of Physics, Chemistry and Biology, Division of Chemistry, Linköping University, SE-58183 Linköping, Sweden

[2] Northeast Structural Genomics Consortium and Ontario Cancer Institute, University Health Network, Toronto, Ontario, Canada

[3] Structural Genomics Consortium, Northeast Structural Genomics Consortium, Ontario, Canada

[4] Cancer Institute and Department of Medical Biophysics, University of Toronto, Ontario, Canada

[#] These authors contributed equally to this work.

Abstract

In this paper, we describe the structure of a novel, unique N-terminal domain motif in the nuclear $FKBP25_{1-73}$, a member of the FKBP family, together with the structure of a sequence-related subdomain of the E3 ubiquitin ligase HectD1 which we show belongs to the same fold. This novel motif adopts a compact 5-helix bundle which we name the BTHB (Basic Tilted Helix Bundle) domain. A positively charged surface patch, structurally centered around the tilted helix H3, is present in both FKBP25 and HectD1 and is evolutionary conserved for both proteins, suggesting a conserved functional role. By detailed comparative analysis of the structures of the two proteins and their sequence similarities, and by analyzing the interaction of the proposed FKBP25 binding protein YY1, we suggest that the basic motif in BTHB is involved in the observed DNA binding of FKBP25, and can be affected by regulatory YY1 binding and/or interactions with adjacent domains.

INTRODUCTION

FK506-binding proteins (FKBPs) belong to the family of the immunophilins first defined by their joint property of binding immunosuppressant drugs such as FK506 and rapamycin [1]. The conserved binding site for the immunosuppressant drugs is located in the common peptidylprolylcis/trans isomerase (PPIase) domain, where drug binding hampers further interactions with proteins such as calcineurin and mTOR leading to decreased T cell proliferation[1, 2]. The PPIase domain in FKBPs can occur singly or in multiple copies, and

[*]To whom correspondence should be addressed: maria.sunnerhagen@liu.se, Department of Physics, Chemistry and Biology, Division of Chemistry, Linköping University, SE-58183 Linköping, Sweden; Tel: +46-13-286682; Fax: +46 13 13 75 68..
[5]Current affiliation: Department of Cancer Biology, Dana-Farber Cancer Institute, Boston, Massachusetts 02215, USA
[6]Current affiliation: Department of Medical Sciences, Molecular Medicine and Science for Life Laboratory, Uppsala University, Uppsala, 75123 Sweden
[7]Current affiliation: Max-Planck-Institut für Kohlenforschung, Kaiser-Wilhelm-Platz 1, 45470 Mülheim and der Ruhr, Germany

is flanked by various other modules and/or sequence motifs depending on function and cellular localization[2]. The first of the immunophilins discovered in the nucleus was FKBP3[3], now predominantly known as FKBP25, which is the name we will use throughout[2, 4].

Compared to other multidomain proteins in this family, FKBP25 is a small (25 kDa) FKBP with only two domains: a C-terminal PPIase domain, and an N-terminal basic domain unique for mammalian FKBPs. Whereas the structure of its C-terminal PPIase domain was solved in complex with rapamycin[5](PDB id 1PBK), the N-terminal domain, with hitherto unknown structure, was found to bind both nucleolin/C23[6] and DNA[7]. By analogy with FKBPs in plants and yeast which contain nucleolin-like domains and thereby may have similar functions as nucleolin in chromatin remodeling[8], the N-terminal domain of FKBP25 has been suggested to have a role in regulating the association state of nucleosomes by interacting with nucleolin[4]. Moreover, this basic domain in FKBP25 forms alternative complexes with other chromatin-related proteins, such as the HDAC1, HDAC2, and the transcriptional regulator YY1, the DNA binding activity of which is enhanced on binding FKBP25[9].

Human HectD1 is a 2612-residue HECT superfamily E3 ubiquitin ligase containing 4 recognizable domains: ANK repeats, a SAD domain, a MIB/HERC2 domain, and a HECT E3 ligase domain. HectD1 knockout mice show perinatal lethality, exencephaly, impaired neural fold elevation, abnormal head mesenchyme morhology, and defects in eye and cranial vault morphology (11). Cell studies suggest that the Adenomatous Polyposis Coli (APC) protein is modified at Lys-63 by HectD1 with polyubiquitin to promote APC-Axin interaction, with effects on the cell fate and homeostasis[10]. Moreover, HectD1 ubiquitination regulates intracellular localization and secretion of Hsp90 to promote correct neural tube closure in mice [11].

During our structural genomic efforts, we discovered an additional domain within HectD1, between residues 1879-1966. Interestingly, we found that the fold of this domain is similar to that of the N-terminal domain of FKBP25. Here we present these two structures: the N-terminal domain $FKBP25_{1-73}$, and the sequence-wise distant but structure-wise similar domain of $HectD1_{1879-1966}$. Although the function of these domains remains unknown, by comparing the two structures and their sequence conservation, and by performing the additional ligand titration with the proposed FKBP25 binding protein YY1, we put forward a hypothesis on the location of interaction surfaces that are shared and not shared between FKBP25 and HectD1.

METHODS

Cloning, expression, and purification

The N-terminal residues 1-73 of FK506 binding protein 3, 25kDa (FKBP3, also known as FKBP-25; PPIase) was cloned from a Mammalian Gene Collection cDNA template (fkbp03.BC020809.MGC.AU84-G12.pDNR-LIB) and region 1881-1968 of HECT domain containing 1 (HectD1) was cloned from a Kazusa cDNA template (hectd1.BAA86445.KZA.KIAA1131.pBluescriptSK+) into the pET28aLIC (GenBank,

EF442785) and pET28MHL (GenBank, EF456735) vector, respectively using the In-Fusion CF Dry-Down PCR Cloning Kit (Clontech, 639605).

A 250 ml flask containing M9 base minimum media (with ^{13}C-glucose and ^{15}N $(NH_4)_2SO_4$) supplemented with 50 ug/ ml kanamycin (BioShop Canada KAN 201) was inoculated from a fresh transformed plate of BL-21(DE3) CodonPlus. The flask was shaken overnight (16 hours) at 250 rpm at 37°C. Using the Lex system, a 2L bottle (VWR 89000-242) containing 1800 ml of minimum media supplemented 50 μg/ ml kanamycin and 600 μl antifoam 204 (Sigma A-8311) was inoculated with 50 ml overnight LB culture, and incubated at 37°C. The temperature of the media was reduced to 15°C one hour prior to induction and induced at $OD_{(600)}$ = 2 with 100 μM isopropyl-thio-b-D-galactopyranoside (BioShop Canada IPT 001). Cultures were aerated overnight (16 hours) at 15°C, and cell pellets collected by centrifugation and frozen at −80 °C.

Frozen cell pellet contained in bags (Beckman 369256) obtained from 2L of culture were thawed by soaking in warm water. Each cell pellet was resuspended in 25-40 mL lysis buffer and homogenized using an Ultra-Turrax T8 homogenizer (IKA Works) at maximal setting for 30-60 seconds per pellet. Cell lysis was accomplished by sonication (Virtis408912, Virsonic) on ice: the sonication protocol was 10 sec pulse at half-maximal frequency (5.0), 10 second rest, for 10 minutes total sonication time per pellet. Unclarified lysate was mixed with 2-3 mL of Ni-NTA superflow Resin (Qiagen) per 40 mL lysate. The mixture was incubated with mixing for at least 45 minutes at 4°C. The mixture was than loaded onto an empty comlum (BioRad) and washed with 100 ml wash buffer. Samples were eluted from the resin by exposure to 2-3 column volumes (approx. 10-15 mL) of elution buffer. An XK 26x65 column (GE Healthcare) packed with HighLoad Superdex 75 resin (GE Healthcare) was pre-equilibrated with gel filtration buffer for 1.5 column volumes using an AKTA explorer (GE Healthcare) at a flow rate of 2.5mL/min. The eluate sample from the IMAC step (approx. 15 mL) was loaded onto the column at 1.5 mL/min, and 2mL fractions were collected into 96-well plates (VWR 40002-012) using peak fractionation protocols). Fractions observed by a UV absorption chromatogram to contain the protein were pooled. Purified proteins were concentrated using 15 mL concentrators with a 5,000 molecular weight cut-off (Amicon Ultra-15, UFC900524, Millipore) at 3750 rpm, typically resulting in a final concentration of 4-5 mg/mL. Lysis buffer: 1× PBS, 250 mM NaCl, 5 mM imidazole, 1mM phenylmethane-sulfonyl fluoride, and 100 mL Sigma general protease inhibitor (Sigma P2714-1BTL, resuspended according to manufacturer's instructions)); Wash buffer: 1x PBS, 250 mM NaCl, 20 mM imidazole; Elution buffer: 1x PBS, 250 mM NaCl, 250 mM imidazole; Gel filtration buffer: 1x PBS, 250 mM NaCl, 2 mM DTT.

The Pet28-MHL vector containing the gene for the his-tagged $YY1_{293-350}$, comprises the proposed FKBP25 interaction site $YY1_{300-333}$ [9] but slightly extended c-terminally to include two complete zinc fingers [12] (PDB id 1UBD).E. coliBL21(DE3)pLysS cells were transformed using electroporation, cultured at 37°C in 2 liters of LB-Kan-Cam and induced with 1 mM IPTG at OD_{600} = 1.0, jointly with adding10 μM $ZnCl_2$. The cells were incubated at 22°C overnight, harvested by centrifugation at 4°C, and the pellet resuspended in lysis buffer at pH 8.0 (50 mM NaH_2PO_4, 300 mMNaCl, 10 mM imidazole, 10 mM β-merchaptoethanol; with complete protease inhibitor (Roche)), lysed by sonication and

centrifuged at 13000g, 4°C, 30 minutes. The YY1 protein was purified from the supernatant using cobalt-charged TALON metal affinity resin (Clonetech) washed prior- and post sample loading with 15 column volumes of lysis buffer. Elution was performed stepwise in lysis buffer, pH 8.0,with 20-250 mM imidazole. Fractions containing$YY1_{293\text{-}350}$ as judged from SDS-PAGE were dialysed against gel filtration buffer (10 mMTris, 300 mMNaCl, 10 mM DTT, pH7.0) and separated from residual impurities on a HiLoad 16/60 Superdex 75 gelfiltration column (GE Healthcare).

NMR spectroscopy

NMR spectra were recorded at 25°C on Varian Inova 600, BrukerAvance 600 MHz or 800 MHz spectrometers equipped with cryoprobes.Both structures were determined in a streamlined, integrated strategy using a limited set of non-uniformly sampled 3D NMR spectra, ABACUS, and CYANA[13]. For both proteins, HNCO, CBCA(- CO)NH, HBHA(CO)NH, HNCA, (H)CCH-TOCSY and H(C)CH-TOCSY, ^{15}N-edited NOESY-HSQC (t_m = 100 ms), and ^{13}C-edited aliphatic and aromatic NOESY-HSQC and TOCSY-HSQC in H_2O (t_m = 100 ms) spectra were employed, where peak picking was performed manually using Sparky[14]. NOESY peaks were assigned in iterative cycles of automated structure calculation and NOE assignment USING CYANA 2.0[15]. For FKBP25, anisotropic media for measurement of dipolar couplings was prepared by addition of filamentous phages (Pf1) (ASLA Biotech, Riga) to a concentration of 5mg/ml. The ^{1}J and ^{1}J $+^1$D splittings were measured under isotropic and anisotropic conditions, respectively, on an AV600 Bruker instrument equipped with a cryogenically-cooled probehead with the experiments 2D IPAP-^{1}H-^{15}N HSQC (for $^1J(+^1D)_{HN}$) [16], 3D HNCO-IPAP (for $^1J(+^1D)$ and $^1J(+^1{}_{CaCo}\ D)_{HNCa}$) and 3D HNCO-IPAP (for $^1J(+^1D)_{NCo}$) [17] using time-optimized strategies, when advantageous, such as Band-selective Excitation Short-Transient (BEST) for rapid repetition [18] or non-uniform sampling (NUS) with multidimension decomposition (MDD) for sparse acquisition [19]. A total of 293 RDCs (68HN, 56 CaCo, 56HCa and 63 NCo) were extracted of which 138 were retained for final structure refinement based on small error estimation and secondary structure elements. The RDC fit to the structure was analysed using PALES [20]. The final 20 lowest-energy structures were refined with the CNS [21] package by performing a short constrained molecular dynamics simulation in explicit solvent[22]. Resulting structures were analyzed using the PSVS validation software[23]. The final refined ensembles of 20 structures and resonance assignments for $FKBP25_{1\text{-}73}$ and $HectD1_{1879\text{-}1966}$were deposited into the Protein Data Bank and BioMagRes DB with accession codes 2KFV, 16189 and 2LC3, 17594, respectively. Chemical shift perturbations (CSPs) for $FKBP25_{1\text{-}73}$ were measured from HSQCs on adding unlabeled $YY1_{293\text{-}350}$ to 300 μMFKBP$25_{1\text{-}73}$ up to three-fold excess of YY1, in 10 mMTris 300 mMNaCl, 10 mM DTT and 187 μM $ZnCl_2$ (higher amounts led to precipitation). Background minor CSPs from $ZnCl_2$ addition to FKBP3 alone were corrected for. In the absence of Zn^{2+}, no CSPs were observed.

Bioinformatic evaluation

ConSurf was used to structurally analyze conserved regions of $FKBP25_{1\text{-}73}$ and $HectD1_{1879\text{-}1966}$. ConSurf uses a multiple sequence alignment to map the level of conservation upon the protein structure[24, 25]. The multiple sequence alignment was

created by MUSCLE v3.8 using sequence homologs to $FKBP25_{1\text{-}73}$ and $HectD1_{1879\text{-}1966}$. The homologs were identified by running Blastp against the protein sequence database NR, choosing one representative sequence for each species. The sequence for fkbp3 was extracted from Refseq using accession number NP_002004.1 and accession number BAG54248.1 was used for HectD1 (GenBank).

RESULTS AND DISCUSSION

The coordinates of the NMR structure of $FKBP25_{1\text{-}73}$, comprising the 8.4 kDa N-terminal domain of the full-length protein, as presented here (**Fig. 1**) were deposited in the PDB as 2KFV and its resonance assignment in the BioMagResBank (BMRB) as entry 16189. The statistics for the NMR structure, comprising an ensemble of the 20 lowest energy conformers, are reported in Table 1. The N-terminal domain of FKBP25 was originally predicted as a Helix-Loop-Helix motif, characteristic of transcription factors and DNA-binding proteins [26], with the two helices corresponding to residues 7-19 and 33-50 and linked by a loop [7]. In contrast, the $FKBP25_{1\text{-}73}$ structure (**Fig. 2a**) shows an entirely different fold where the two predicted helical regions present five structurally distinct but well-bundled helices (H1: 11-17; H2: 22-33; H3: 34-41; H4: 46-52; H5: 55-70). The secondary structure elements are wrapped around a joint hydrophobic core, created with a substantial contribution of the aliphatic amino acids alanine and leucine, which are present in a high number in the sequence (11% for alanine and 11% for leucine). Only the four alanines at the disordered N-terminal end do not participate in the core. The other amino acid type highly present in the sequence is lysine (12.3%), which confers the basic nature to this domain, with a pI of 9.63. In particular, 6 out of 9 lysines (K22, K23, K27, K48, K52 and K56) are closely localized in the structure, thereby creating a continuous positive patch comprising H2, the N-terminal end of H5, and H4 (**Fig. 2b**).A ConSurf analysis where the conservation of the protein sequence is mapped onto the structure showed only one continuous conserved surface patch including residues K22, K23, N49, K52, T53 and K56 (Fig. 2c), highly conserved over a wide range of species ranging from sea anemones to human. The spatial overlap of this conserved surface region with the positive surface patch indicates an evolutionary conserved functional role. The positive charge of this motif together with its protruding shape renders complementarity to a major groove, thus likely accounting for the DNA binding activity of the N-terminal domain of FKBP25[7].

To molecularly map the interaction of $FKBP25_{1\text{-}73}$with YY1 that had been identified previously[9], CSPs on ^{15}N-labelled $FKBP25_{1\text{-}73}$were measured in HSQC titrations with unlabeled $YY1_{293\text{-}350}$, comprising the proposed FKBP25 interaction site $YY1_{300\text{-}333}$ [9]. Only $FKBP25_{1\text{-}73}$ residues A3, E31, H32, L38 and K73 were found to show significant $YY1_{293\text{-}350}$ –dependent CSPs in the presence of Zn^{2+}, ranging from 0.05 to 0.12 ppm; notably, these residues were positioned in the same region of the domain, distant from the positively charged surface described above (**Fig. 2c**). Only residue L38 in this patch is conserved between $FKBP25_{1\text{-}73}$ and $HectD1_{1879\text{-}1966}$, suggesting that the YY1 binding site is not preserved in HectD1. However, since the interaction surface of YY1 and the positive, possibly DNA-binding, surface do not overlap structurally (**Fig. 2c**), the enhanced DNA binding activity of YY1 on binding FKBP25 [9] could be due to allosteric effects and/or YY1 recruitment of an additional DNA-binding motif in FKBP25.

The only other protein sequence with any similarity to $FKBP25_{1-73}$ as identified by a wide BLAST search comprised a subdomain of HectD1, including residues 1879-1966 in human. To find out if this domain had the same fold as $FKBP25_{1-73}$, we determined the structure of $HectD1_{1879-1966}$ by NMR. The structure of the 10 kDa $HectD1_{1879-1966}$ was deposited in the PDB as 2LC3 and in the BMRB as entry 17594. Its core domain aligns to that of $FKBP25_{1-73}$ with a RMSD of 0.796 Å for the backbone and 1.148 for all the atoms (2KFV: 11-70; 2LC3: 1895-1958) with PyMOL [27]. The statistics for the NMR structure of $HectD1_{1879-1966}$ are listed in Table 1, with the 20 lowest energy conformers shown in Figure 1. $HectD1_{1879-1966}$ also shows five core helices as does $FKBP25_{1-73}$, but with an additional small helix N-terminal to the core fold (H0: 1882-1887; H1: 1895-1903; H2: 1909-1921; H3: 1922-1929; H4: 1934-1942; H5: 1943-1958) (**Fig.2d**). Again, this domain holds a high percentage of lysine (12.5%, pI: 8.45), but only 3 lysines out of 11 (K1910, K1936 and K1940, corresponding to K22, K48 and K52 in $FKBP25_{1-73}$ respectively) are grouped closely. Still, together with residues R49, K52 and R64, from H3, H4 and the loop joining them, a wide positively charged surface is created in the same region as in $FKBP25_{1-73}$, but slightly more shifted toward H3 (**Fig. 2e**). The other lysines are spread in sequence and in particular 4 ones are localized in proximity of the N-terminal helix H0. The role of this basic patch, or of the intact $HectD1_{1879-1966}$ domain, is however currently unknown.

To further evaluate the possible uniqueness of the fold and possibly find other members of this fold family we searched for further structural homologs folds using DALI [28]. The only deposited structure with a significant similarity to the N-terminal domain of FKBP25 was indeed $HectD1_{1879-1966}$ (DALI z-score 9.3), where the immediately following hit, the central region of an AAA ATPase, (PDB: 2QW6) had only 4.2 as Z-score and a good structural matching only for the helices 2 and 5; similar results were obtained when using $HectD1_{1879-1966}$ as the initial search motif. These two helices are short (6-8 amino acids) compared to the other helices but their most interesting characteristic is their relative position. While the three other core helices tend to assume more a parallel/bundle-like conformation, these two helices are tilted, with H4 almost perpendicular to H5, and similar relative orientations between H3 and H4 (34° for $FKBP25_{1-73}$ and 38° for $HectD1_{1879-1966}$). It appears that while the relative positions of helices 1, 2 and 5 are similar to what is observed for classic helix bundles, helices comparable to H3 and H4 – which present the tilted basic helix motif - are present only in $FKBP25_{1-73}$ and $HectD1_{1879-1966}$.

Taken together, this work describes the structure of a novel, unique N-terminal domain motif in the FKBP family, $FKBP25_{1-73}$, and its structurally homologous domain $HectD1_{1879-1966}$. In contrast to previous predictions suggesting a HLH motif for this domain [7], the high-resolution structure shows a completely new fold, with the same region predicted to form the HLH motif instead organized in almost four small helices (H1, H2, H3 and part of H4), where H3 and H4 are tilted in a novel arrangement; we call this fold the BTHB (basic tilted helix bundle) domain. Our structural analysis of this fold motif suggests that the DNA binding properties of $FKBP25_{1-73}$ are presented by the conserved basic motif, which is also present in $HectD1_{1879-1966}$. Amino acids participating in $FKBP25_{1-73}$ binding of YY1 are located distant from the DNA binding site, and are not conserved in $HectD1_{1879-1966}$. Structural analysis therefore suggests a fold-uniting basic binding motif,

which could be allosterically fine-tuned by binding of regulatory proteins and/or adjacent protein domains.

REFERENCES

1. Kang CB, et al. FKBP family proteins: immunophilins with versatile biological functions. Neurosignals. 2008; 16(4):318–25. [PubMed: 18635947]
2. Galat A. Functional diversity and pharmacological profiles of the FKBPs and their complexes with small natural ligands. Cell Mol Life Sci. 2013; 70(18):3243–75. [PubMed: 23224428]
3. Jin YJ, Burakoff SJ, Bierer BE. Molecular cloning of a 25-kDa high affinity rapamycin binding protein, FKBP25. J Biol Chem. 1992; 267(16):10942–5. [PubMed: 1375932]
4. Yao YL, et al. FKBPs in chromatin modification and cancer. Curr Opin Pharmacol. 2011; 11(4): 301–7. [PubMed: 21489876]
5. Liang J, et al. Structure of the human 25 kDa FK506 binding protein complexed with rapamycin. Journal of the American Chemical Society. 1996; 118(5):1231–1232.
6. Jin YJ, Burakoff SJ. The 25-kDa FK506-binding protein is localized in the nucleus and associates with casein kinase II and nucleolin. Proc Natl Acad Sci U S A. 1993; 90(16):7769–73. [PubMed: 7689229]
7. Riviere S, Menez A, Galat A. On the localization of FKBP25 in T-lymphocytes. FEBS Lett. 1993; 315(3):247–51. [PubMed: 8422914]
8. Eitoku M, et al. Histone chaperones: 30 years from isolation to elucidation of the mechanisms of nucleosome assembly and disassembly. Cell Mol Life Sci. 2008; 65(3):414–44. [PubMed: 17955179]
9. Yang WM, Yao YL, Seto E. The FK506-binding protein 25 functionally associates with histone deacetylases and with transcription factor YY1. EMBO J. 200120(17):4814–25. [PubMed: 11532945]
10. Tran H, et al. HectD1 E3 ligase modifies adenomatous polyposis coli (APC) with polyubiquitin to promote the APC-axin interaction. J Biol Chem. 2013; 288(6):3753–67. [PubMed: 23277359]
11. Sarkar AA, Zohn IE. Hectd1 regulates intracellular localization and secretion of Hsp90 to control cellular behavior of the cranial mesenchyme. J Cell Biol. 2012; 196(6):789–800. [PubMed: 22431752]
12. Houbaviy HB, et al. Cocrystal structure of YY1 bound to the adeno-associated virus P5 initiator. Proc Natl Acad Sci U S A. 1996; 93(24):13577–82. [PubMed: 8942976]
13. Lemak A, et al. A novel strategy for NMR resonance assignment and protein structure determination. J Biomol NMR. 2011; 49(1):27–38. [PubMed: 21161328]
14. Goddard, TG.; Kneller, DG. SPARKY 3. University of California; San Francisco:
15. Guntert P. Automated NMR structure calculation with CYANA. Methods Mol Biol. 2004; 278:353–78. [PubMed: 15318003]
16. Ottiger M, Delaglio F, Bax A. Measurement of J and dipolar couplings from simplified two-dimensional NMR spectra. J Magn Reson. 1998; 131(2):373–8. [PubMed: 9571116]
17. Permi P, Annila A. Transverse relaxation optimised spin-state selective NMR experiments for measurement of residual dipolar couplings. J Biomol NMR. 2000; 16(3):221–7. [PubMed: 10805128]
18. Schanda P, Van Melckebeke H, Brutscher B. Speeding up three-dimensional protein NMR experiments to a few minutes. Journal of the American Chemical Society. 2006; 128(28):9042–3. [PubMed: 16834371]
19. Orekhov VY, Ibraghimov I, Billeter M. Optimizing resolution in multidimensional NMR by three-way decomposition. J Biomol NMR. 2003; 27(2):165–73. [PubMed: 12913413]
20. Zweckstetter M, Hummer G, Bax A. Prediction of charge-induced molecular alignment of biomolecules dissolved in dilute liquid-crystalline phases. Biophys J. 2004; 86(6):3444–60. [PubMed: 15189846]

21. Brunger AT, et al. Crystallography & NMR system: A new software suite for macromolecular structure determination. Acta Crystallogr D Biol Crystallogr. 1998; 54(Pt 5):905–21. [PubMed: 9757107]

22. Linge JP, et al. ARIA: automated NOE assignment and NMR structure calculation. Bioinformatics. 2003; 19(2):315–6. [PubMed: 12538267]

23. Bhattacharya A, Tejero R, Montelione GT. Evaluating protein structures determined by structural genomics consortia. Proteins. 2007; 66(4):778–95. [PubMed: 17186527]

24. Celniker G, et al. ConSurf: Using Evolutionary Data to Raise Testable Hypotheses about Protein Function. Israel Journal of Chemistry. 2013; 53(3-4):199–206.

25. Ashkenazy H, et al. ConSurf 2010: calculating evolutionary conservation in sequence and structure of proteins and nucleic acids. Nucleic Acids Res. 2010; 38:W529–W533. [PubMed: 20478830]

26. Massari ME, Murre C. Helix-loop-helix proteins: regulators of transcription in eucaryotic organisms. Mol Cell Biol. 2000; 20(2):429–40. [PubMed: 10611221]

27. Schrodinger LLC. The PyMOL Molecular Graphics System, Version 1.3r1. 2010

28. Holm L, Park J. DaliLite workbench for protein structure comparison. Bioinformatics. 2000; 16(6): 566–7. [PubMed: 10980157]

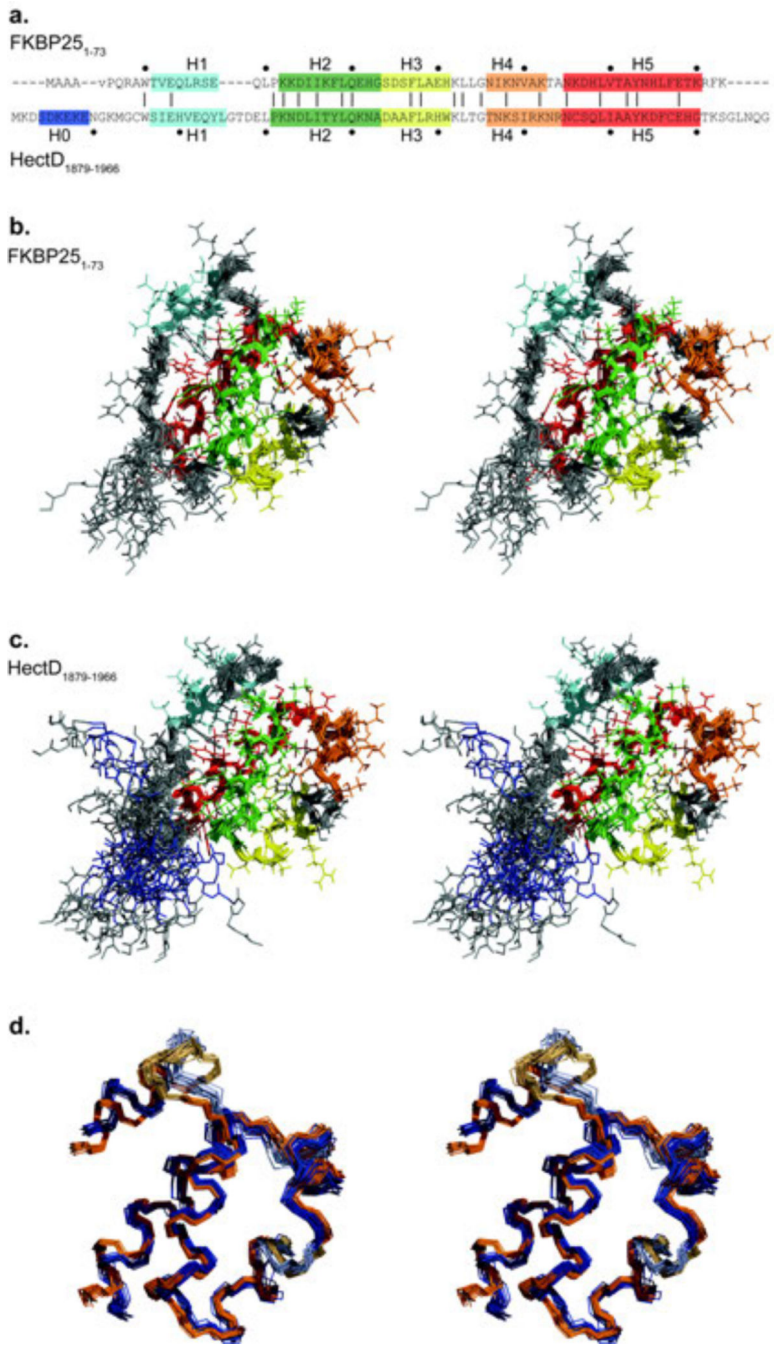

Fig. 1.

Sequence alignment (a) between FKBP25$_{1\text{-}73}$and HectD1$_{1879\text{-}1966}$, with every tenth amino acid in each sequence marked by a dot. Structurally non-equivalent residues (e.g. in loops) are in lowercase. Stereo view of FKBP25$_{1\text{-}73}$ (b) and HectD1$_{1879\text{-}1966}$(c), with the backbone displayed for all the 20 conformers and the side chains only for the lowest energy one, for the sake of clarity. (d) Superimposed backbone representation (oxygen atom of the peptide bond excluded) for FKBP25$_{1\text{-}73}$ (blue) and HectD1$_{1879\text{-}1966}$(orange); the loops are illustrated with in a lihter shade, compared to the helices. (For interpretation of the

references to colours in this figure legend, the reader is referred to the web version of this paper).

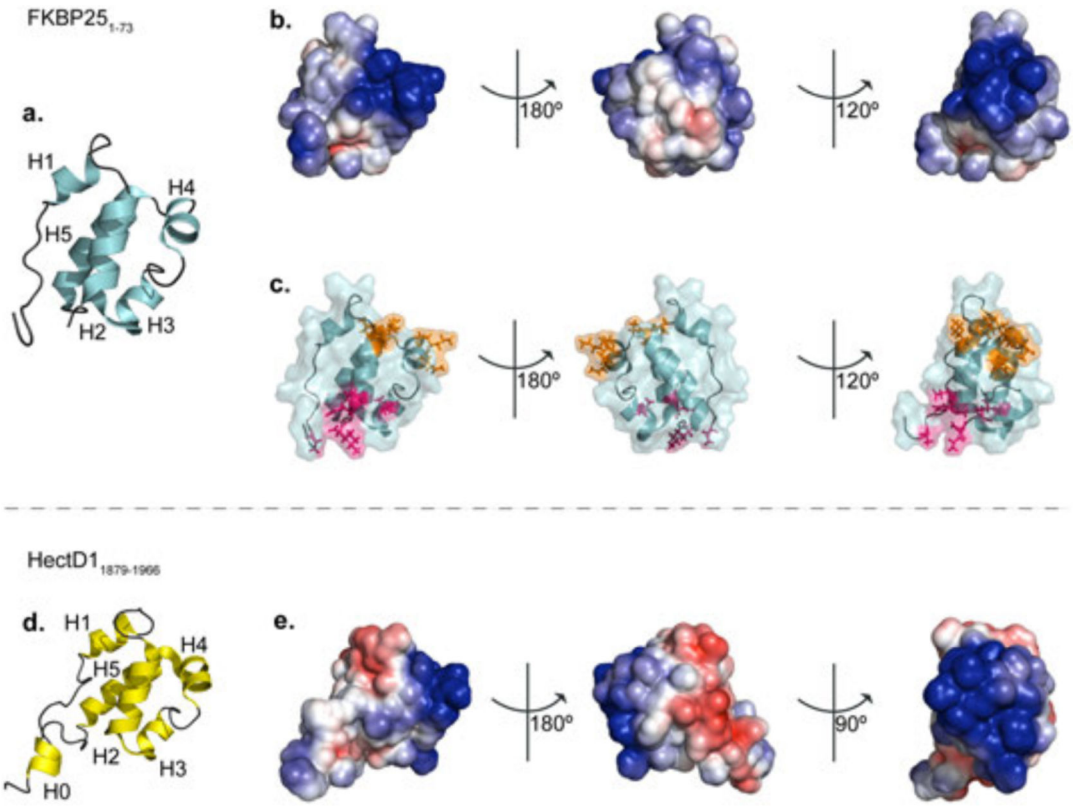

Fig. 2.

Ribbon diagram (a, d) and electrostatics surface (b and e) for the structure of $FKBP25_{1\text{-}73}$ (a and b) and $HectD1_{1879\text{-}1966}$ (d and e), respectively. Surface-exposed, evolutionary conserved residues (orange) and YY1 interaction surface (magenta) are highlighted in (c) for $FKBP25_{1\text{-}73.}$ The electrostatic surface representations were rotated of an appropriate angle in the last view to show in the best way for each structure the wide electrostatic patch. (For interpretation of the references to colours in this figure legend, the reader is referred to the web version of this paper).

Table 1

Structural statistics of the 20 best-fit NMR structures of $FKBP25_{1\text{-}73}$(2KFV) and $HectD1_{1879\text{-}1966}$ (2LC3).

	2KFV	2LC3
A. NMR restraints		
Distance restraints		
Total NOE	1527	2366
Intra residue (|i-j|=0)	740	500
Sequential (|i-j|=1)	435	611
Medium range (2 ≤ |i-j| ≤ 4)	401	632
Long range (|i-j| > 4)	386	623
Hydrogen bonds	28	0
Dihedral angle restraints		
φ	49	76
ψ	49	76
RDC restraints		
$^1D_{NH}$	37	0
$^1D_{NC'}$	51	0
$^1D_{C'C\alpha}$	50	0
B. Structure ensemble statistics		
Violations		
Distance constraints ((>0.5Å)	0	0
Dihedral angle constraints (>10°)	0	0.25±0.43
Deviations from ideal geometry		
Bond lengths (Å)	0.0133±0.0002	0.0135±0.0002
Bond angles (°)	0.899±0.0166	0.891±0.018
Impropers (°)	1.81±0.11	1.84±0.11
Ramachandranplot [b]		
Residues in most favored regions (%)	94.2	89.4
Residues in additionally allowed regions (%)	5.8	10.6
Residues in generously allowed regions (%)	0	0
Residues in disallowed regions (%)	0	0
Average pairwise r.m.s.d.[c] **(Å)**		
Backbone	0.67±0.13	0.47±0.09
Heavy	1.42±0.23	0.96±0.12
Global quality score (Z-score)		
Verify3D	−1.12	−0.80
ProsaII	0.54	1.20
Procheck (phi-psi)	1.02	0.12

	2KFV	**2LC3**
Procheck (all)	−0.06	−1.06
MolprobityClashscore	−0.67	−0.81

[a]Ensemble of 20 lowest-energy structures out of 100 calculated.

[b]Values calculated for the ordered regions, as reported by PSVS [11]: 2LC3, residues 2-7,9-82; 2FKV, residues 27-91.

[c]2LC3, residues 15-79; 2FKV, residues 27-91.